RSC Advances

Synthesis and characterization of glycidyl polymer-based poly(ionic liquid)s: Highly designable polyelectrolytes with poly(ethylene glycol) main chain

T. Ikeda*, I. Nagao, S. Moriyama. J.-D. Kim

Supporting Information

Table of contents

Correspondence Address
Dr. Taichi Ikeda **Polymer Materials Unit** **National Institute for Materials Science** **Namiki 1-1, 305-0044 Tsukuba, JAPAN**

1. IR spectra

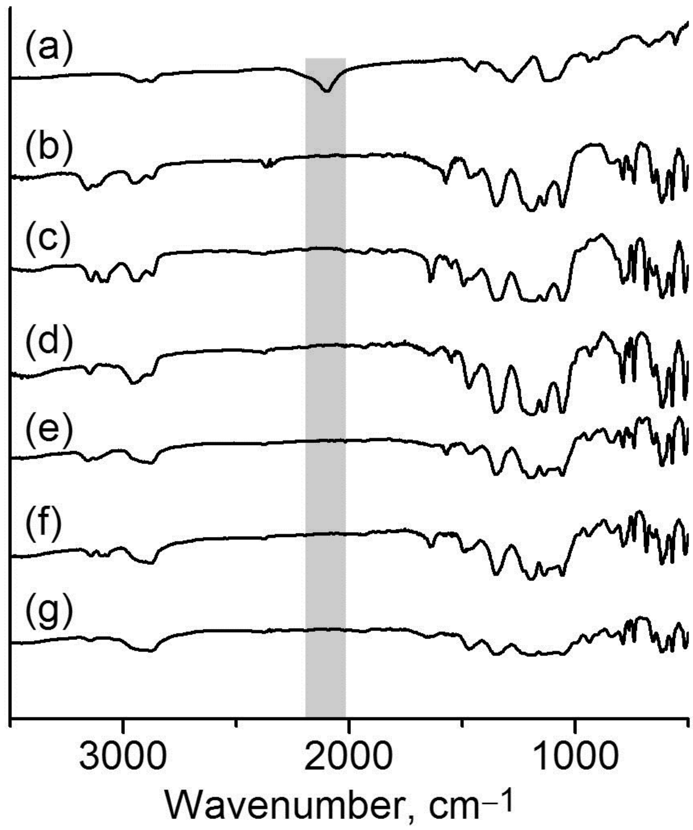

Figure S1. IR data of (a) **GAP**, (b) **GTP-C4-Im·Tf$_2$N**, (c) **GTP-C4-Pyri·Tf$_2$N**, (d) **GTP-C4-Pyrro·Tf$_2$N**, (e) **GTP-EG4-Im·Tf$_2$N**, (f) **GTP-EG4-Pyri·Tf$_2$N**, (g) **GTP-EG4-Pyrro·Tf$_2$N**.
GAP has strong IR peak of azide bond at 2100 cm^{-1}.
No azide bond peak was observed for cationic GTPs

2. ^{1}H and ^{13}C NMR spectra

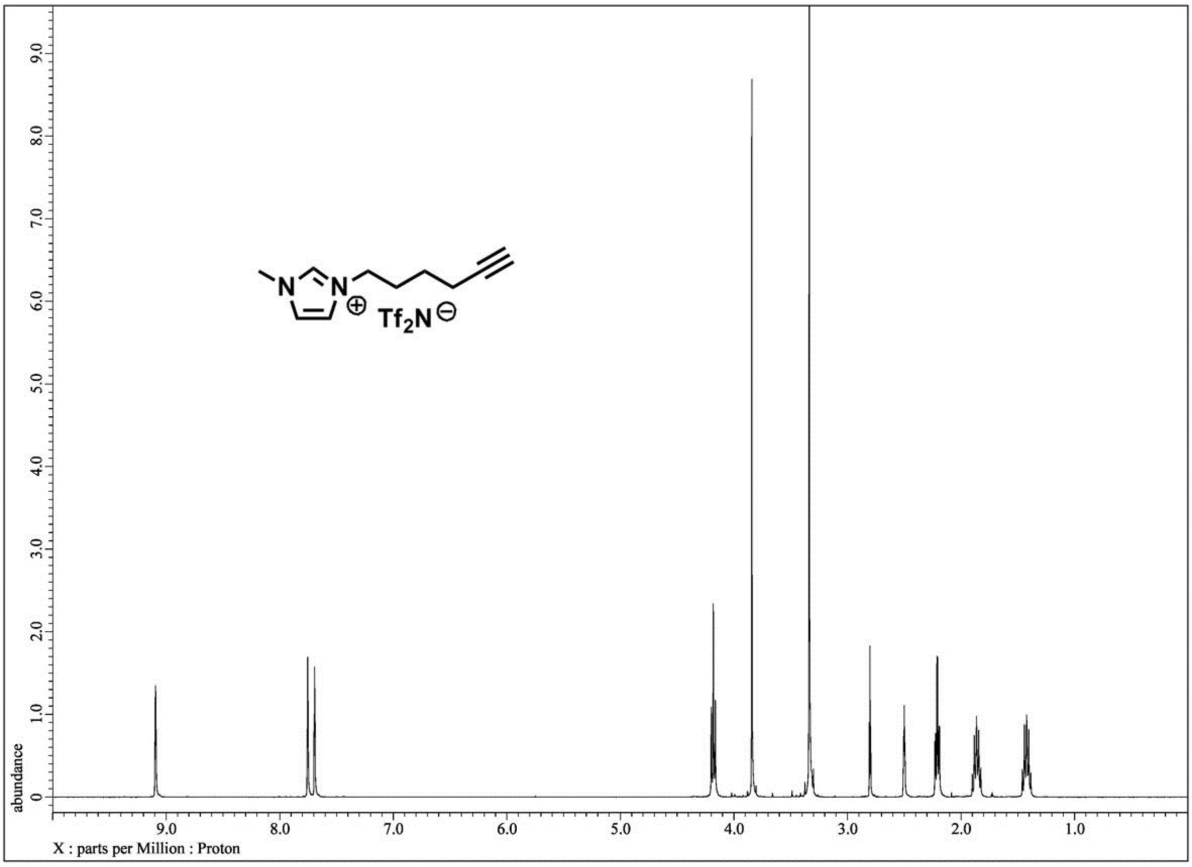

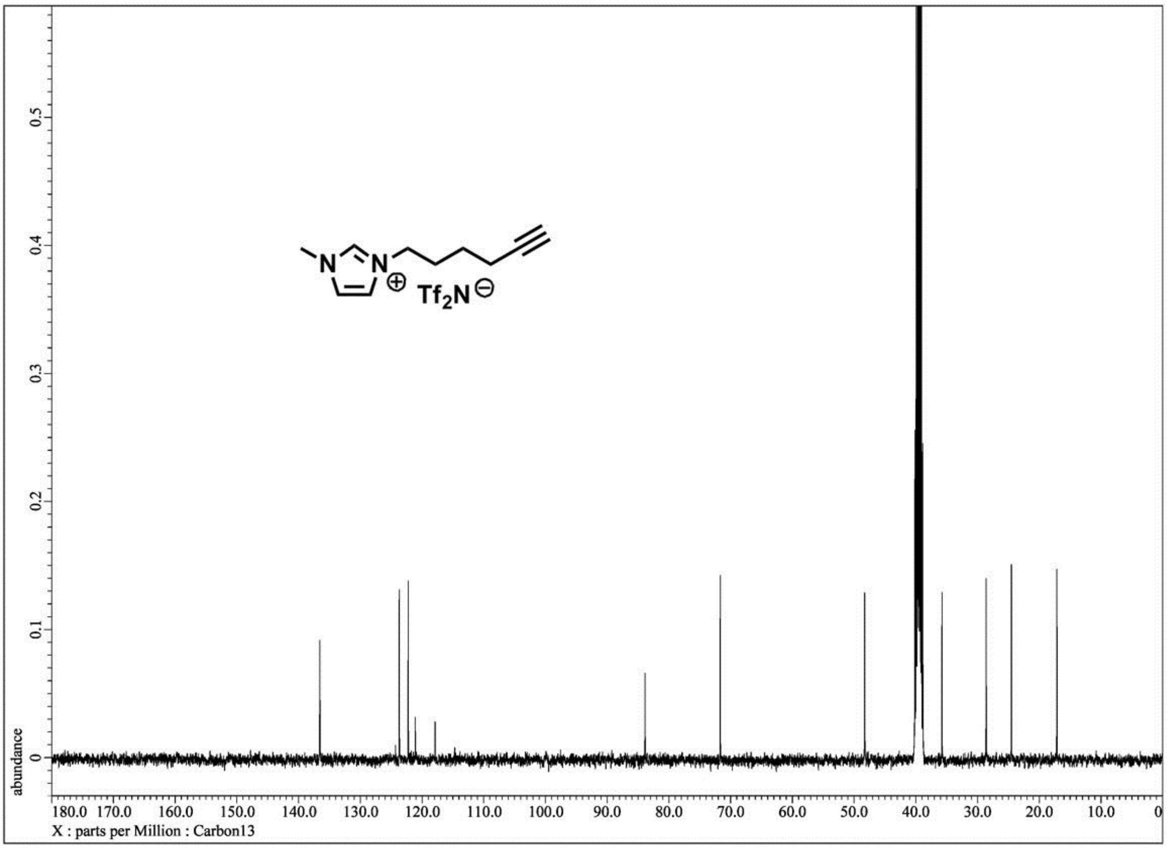

Figure S2. ^{1}H and ^{13}C NMR of **Im-C4-alkyne·Tf$_2$N** (DMSO-d_6).

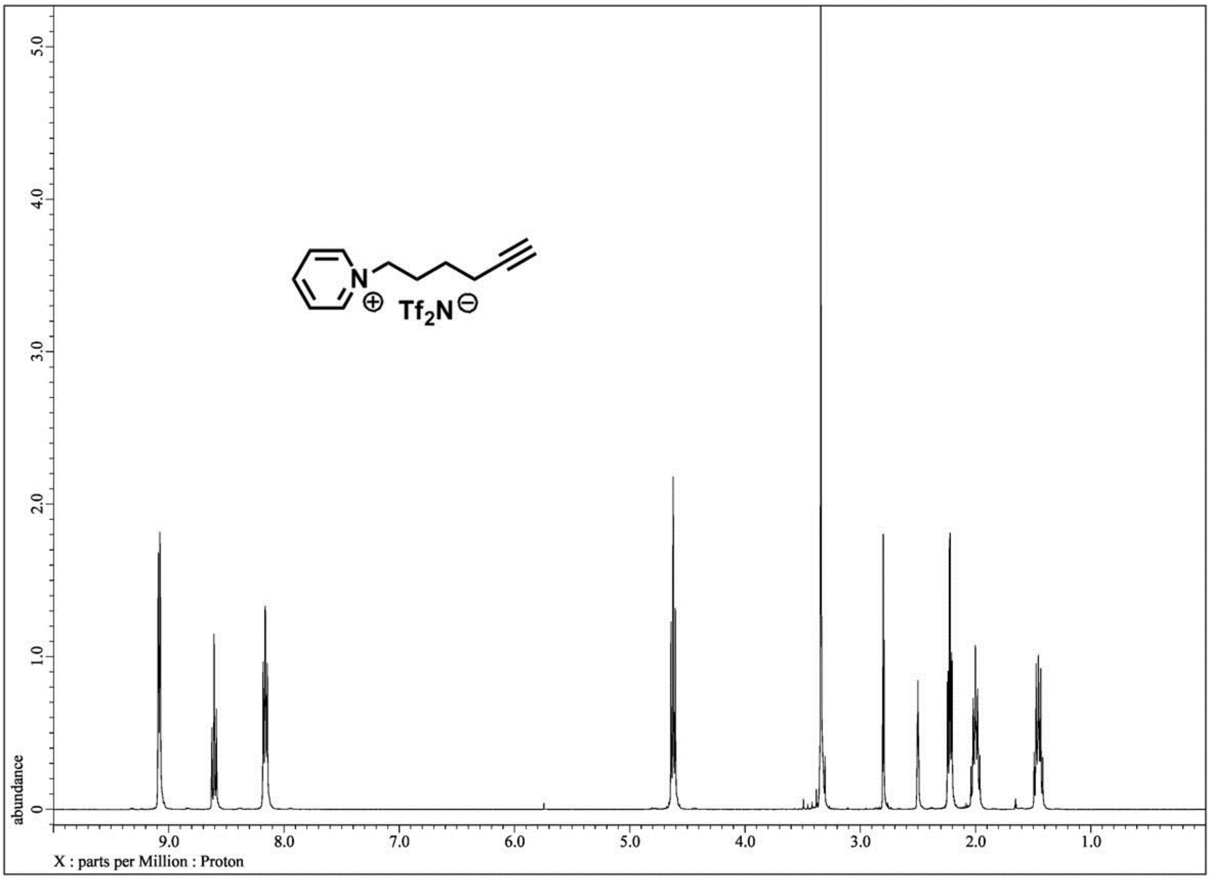

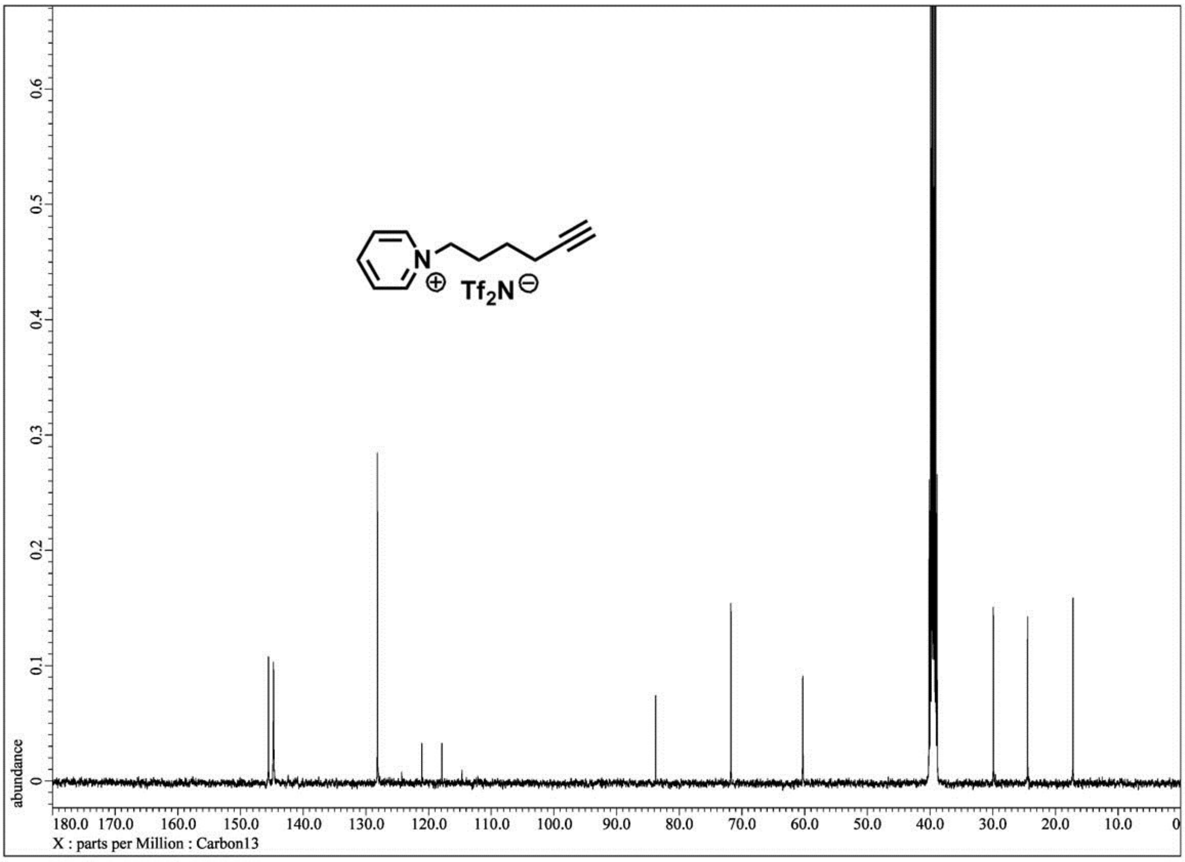

Figure S3. [1]H and [13]C NMR of **Pyri-C4-alkyne·Tf$_2$N** (DMSO-d_6).

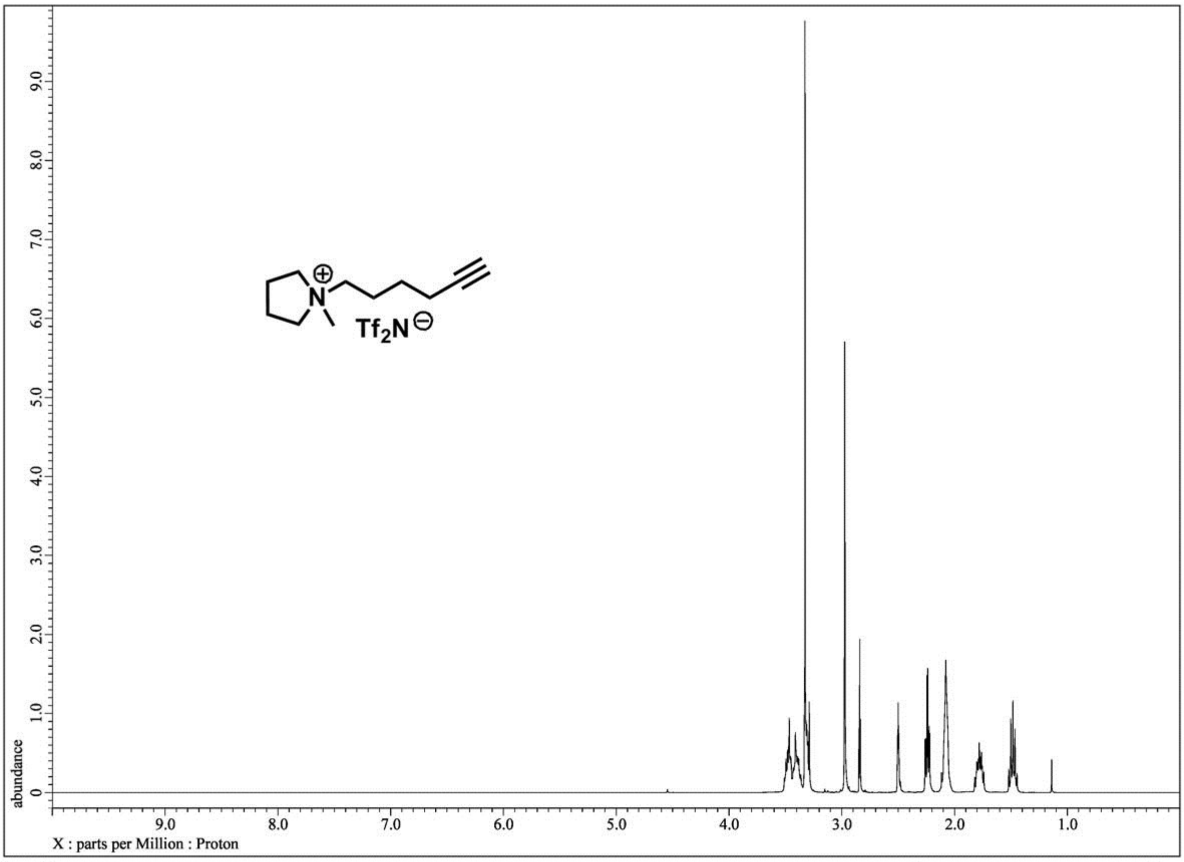

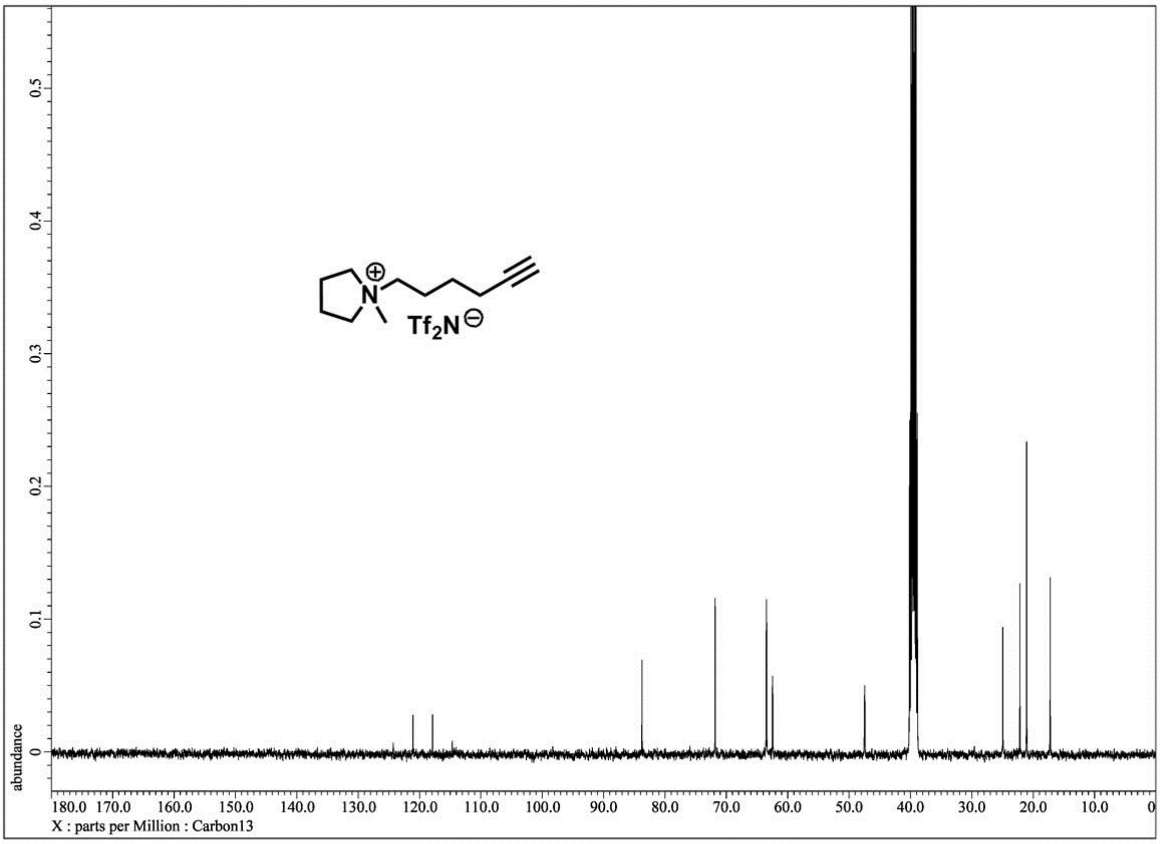

Figure S4. ^{1}H and ^{13}C NMR of **Pyrro-C4-alkyne·Tf$_2$N** (DMSO-d_6).

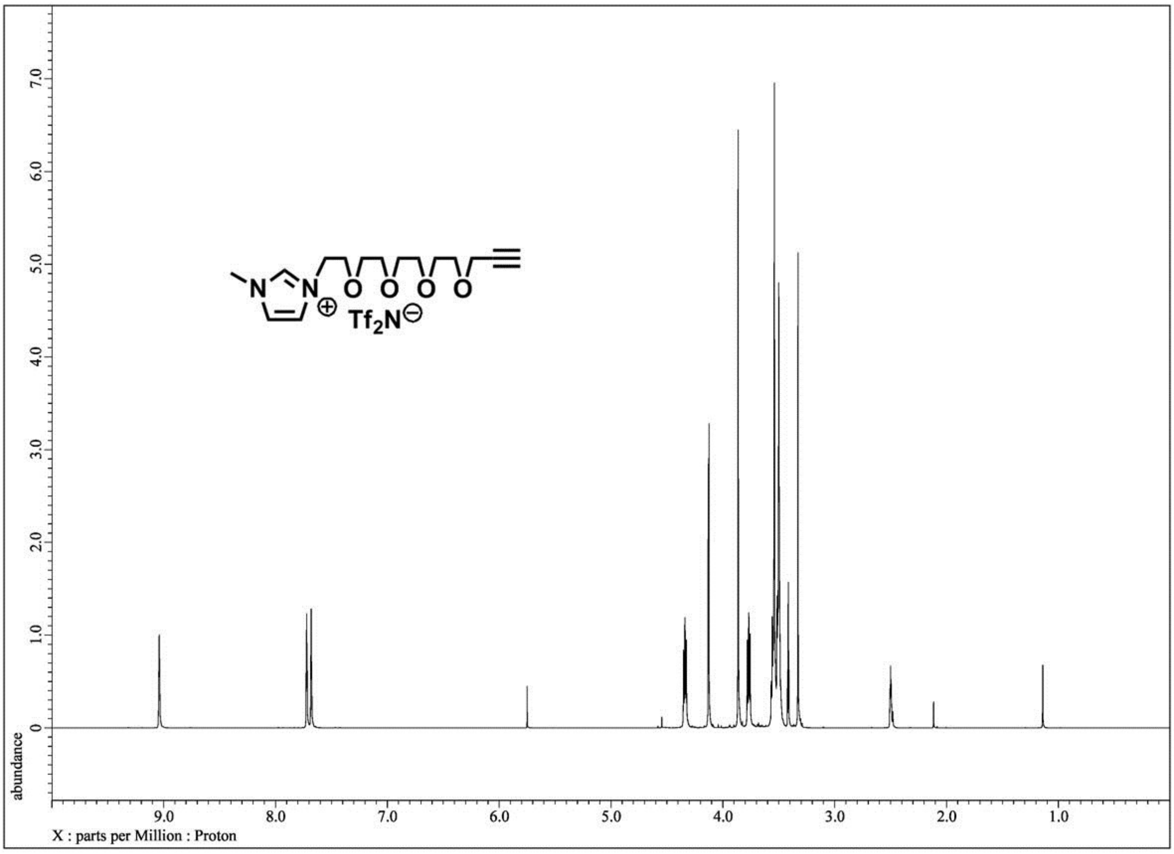

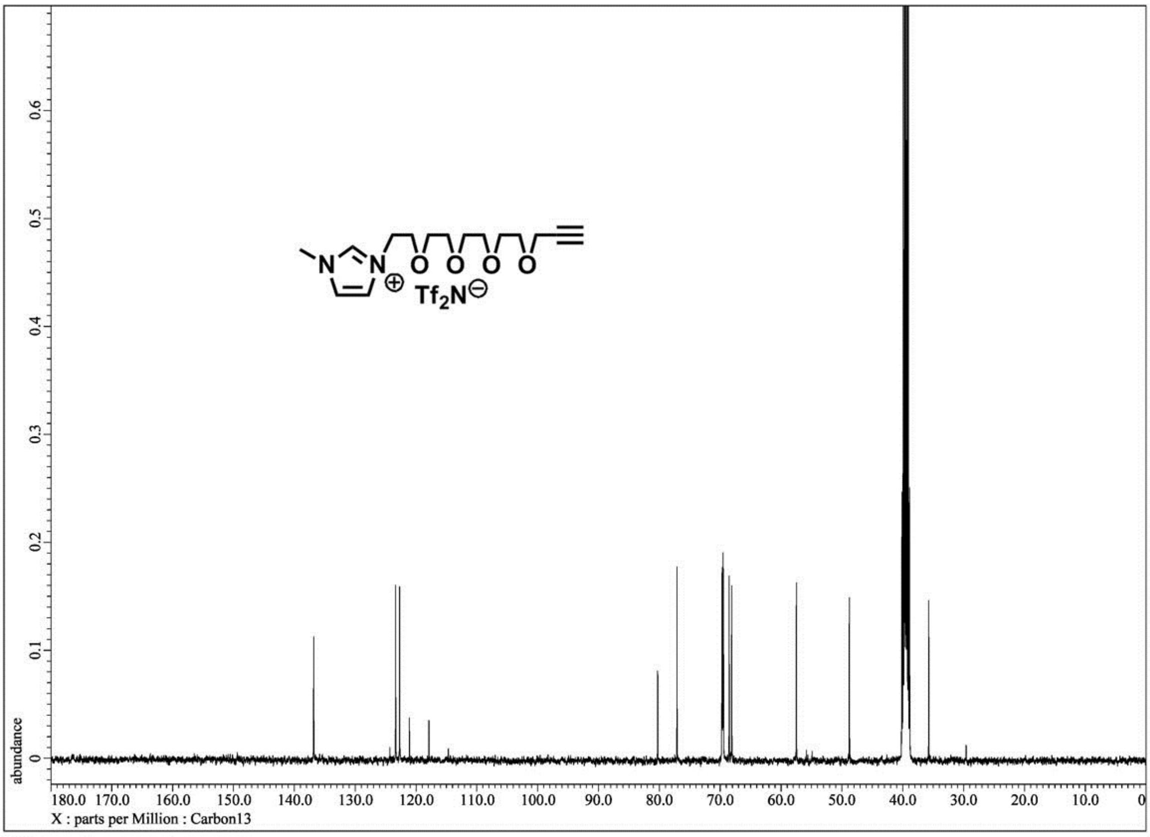

Figure S5. ^{1}H and ^{13}C NMR of **Im-EG4-alkyne·Tf$_2$N** (DMSO-d_6).

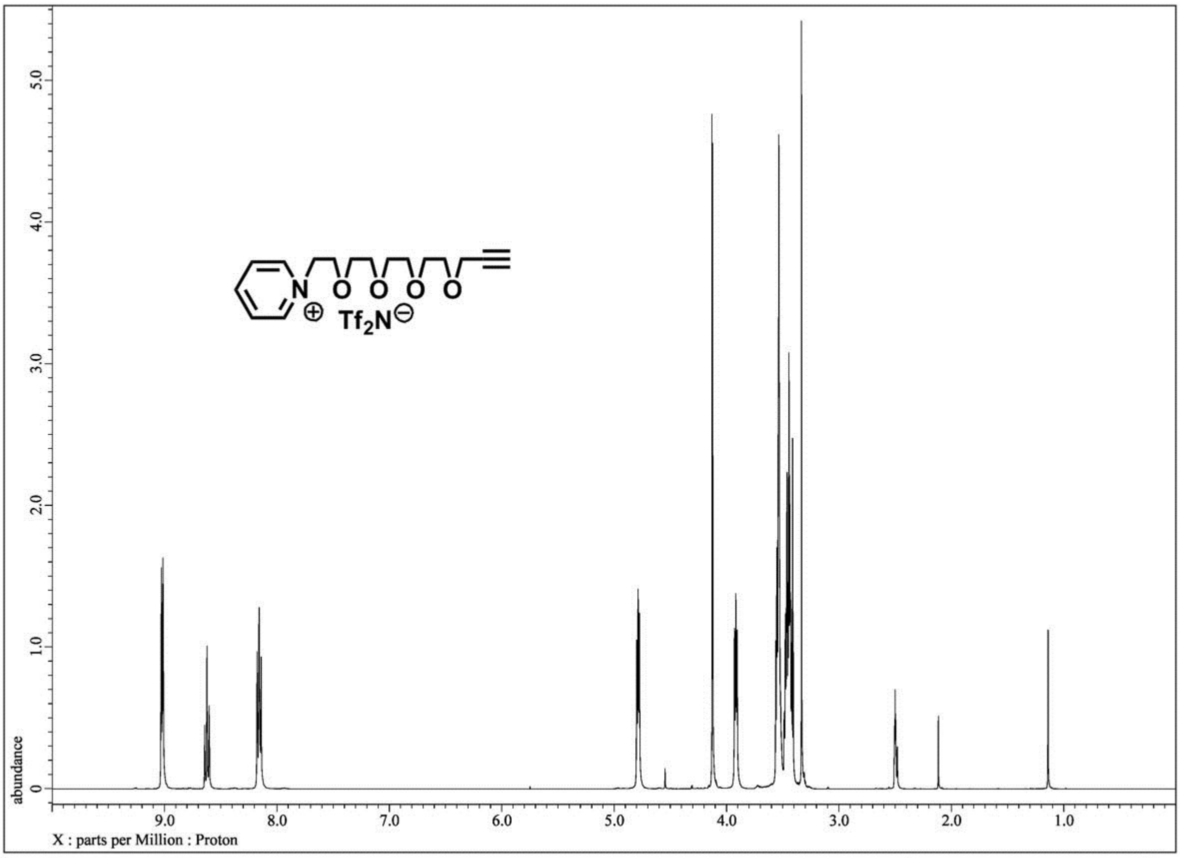

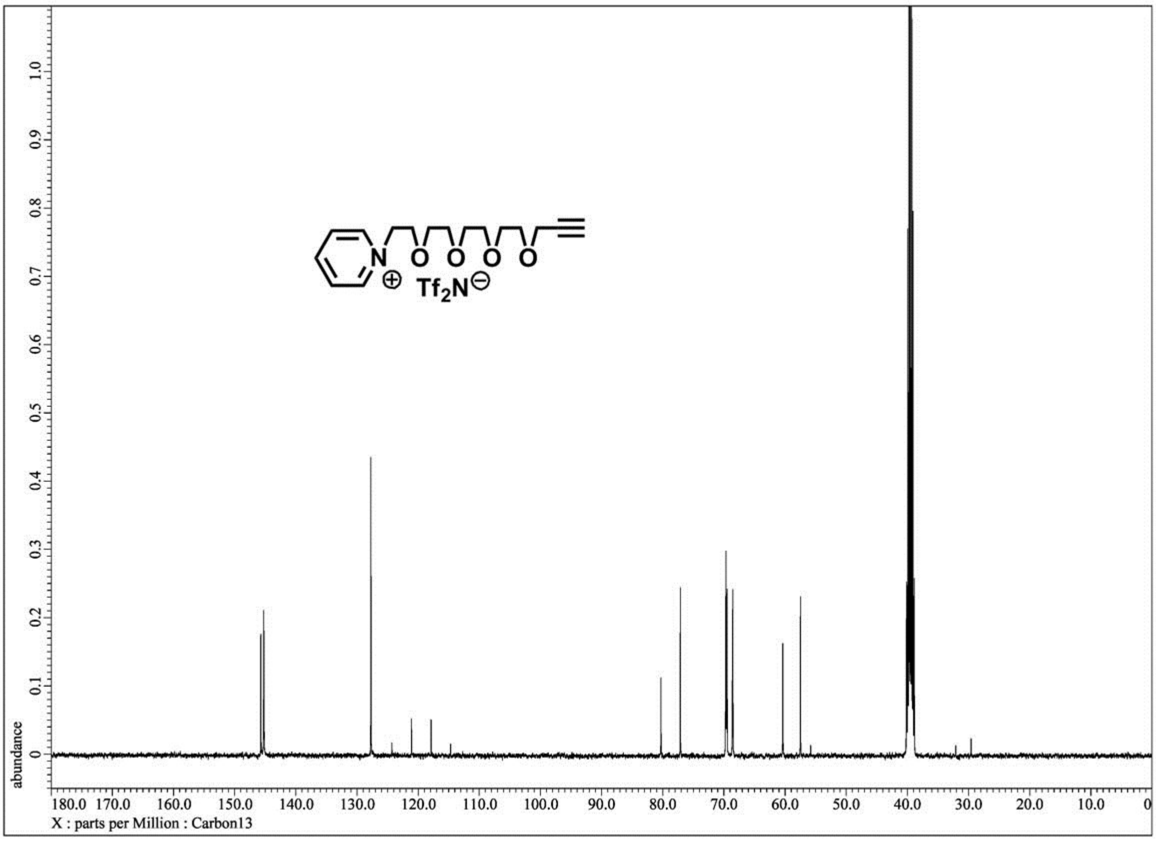

Figure S6. ^{1}H and ^{13}C NMR of **Pyri-EG4-alkyne·Tf$_2$N** (DMSO-d_6).

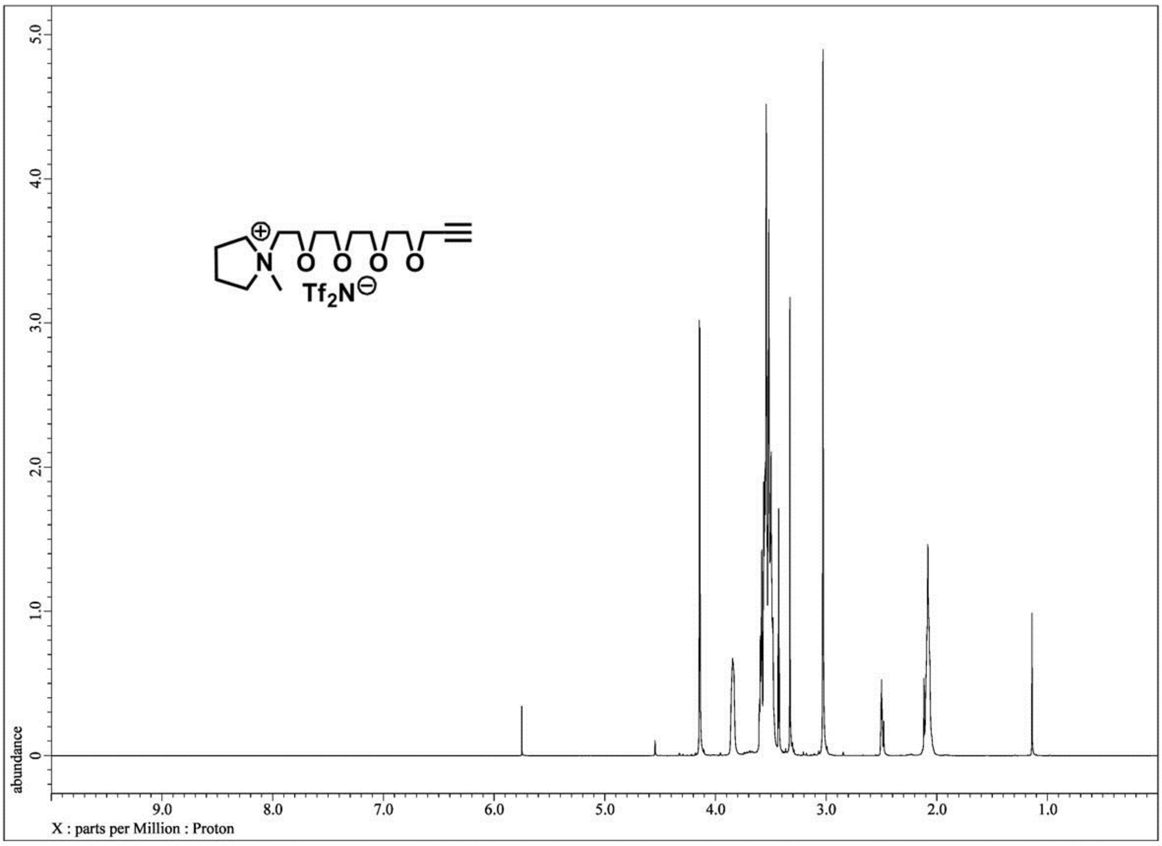

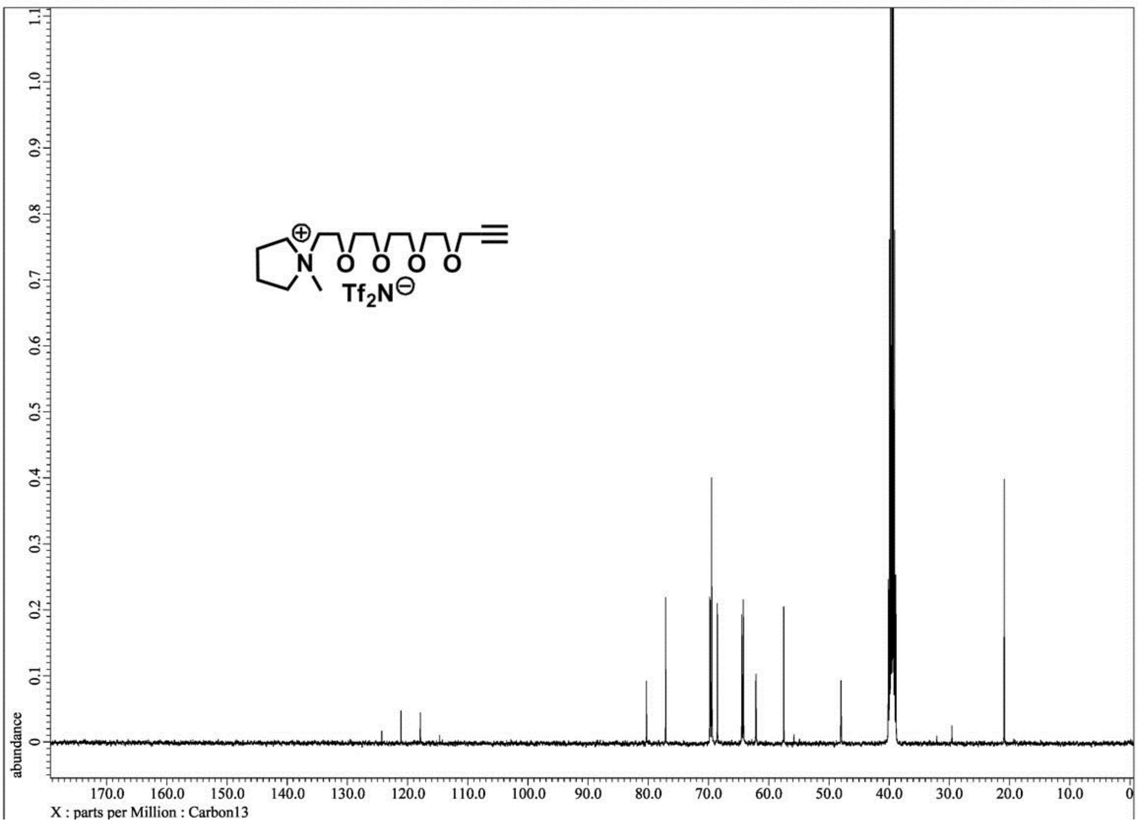

Figure S7. [1]H and [13]C NMR of **Pyrro-EG4-alkyne·Tf$_2$N** (DMSO-d_6).

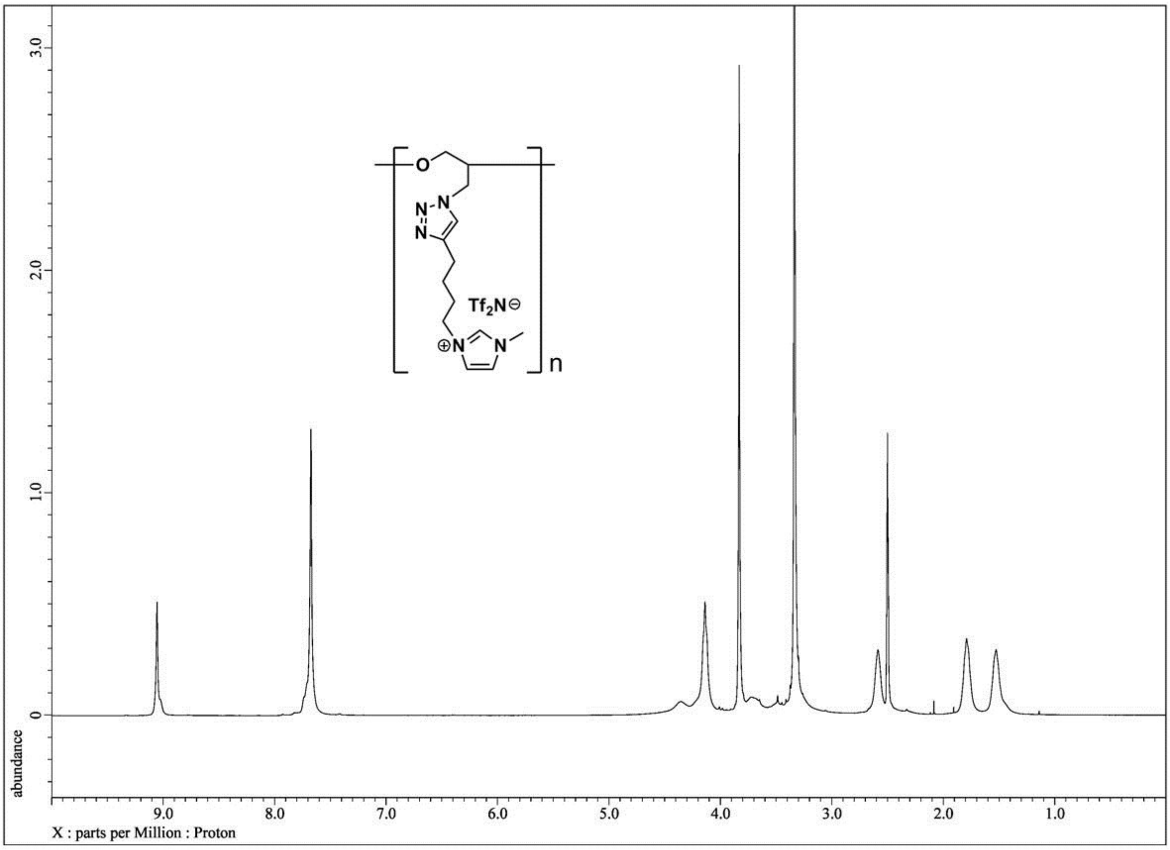

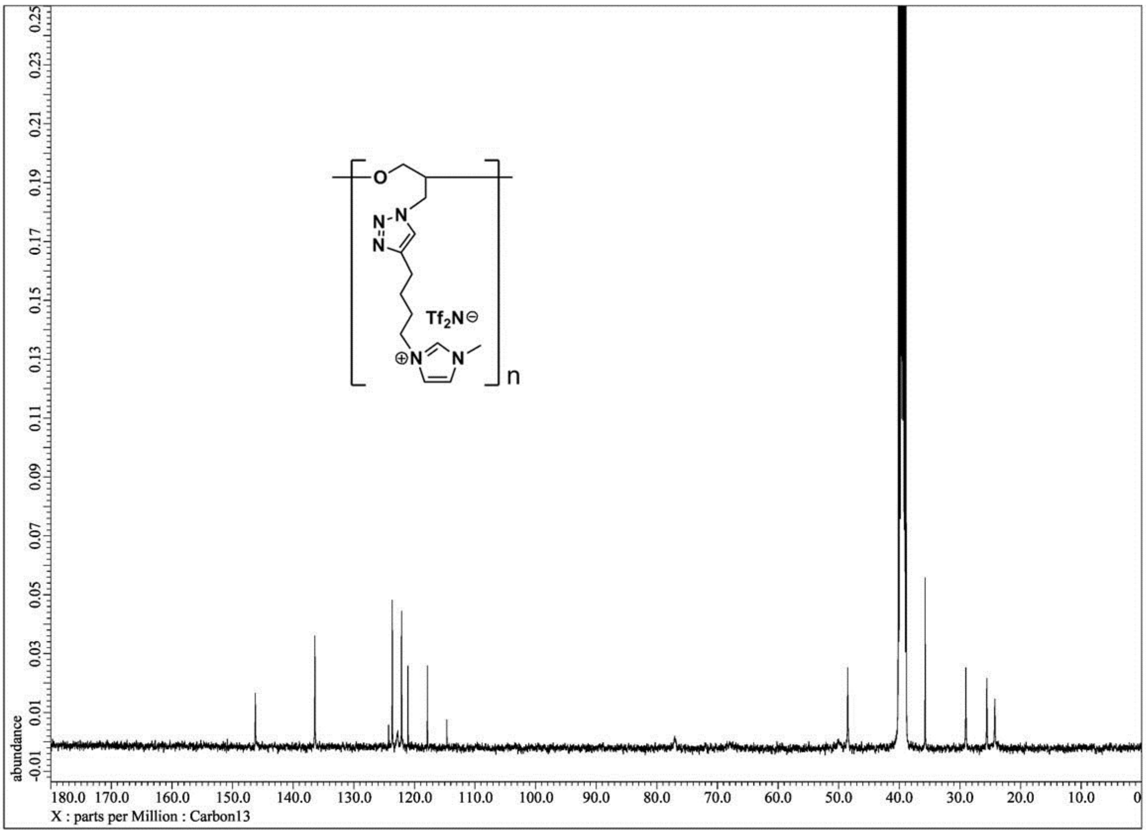

Figure S8. ^{1}H and ^{13}C NMR of **GTP-C4-Im·Tf$_2$N** (DMSO-d_6).

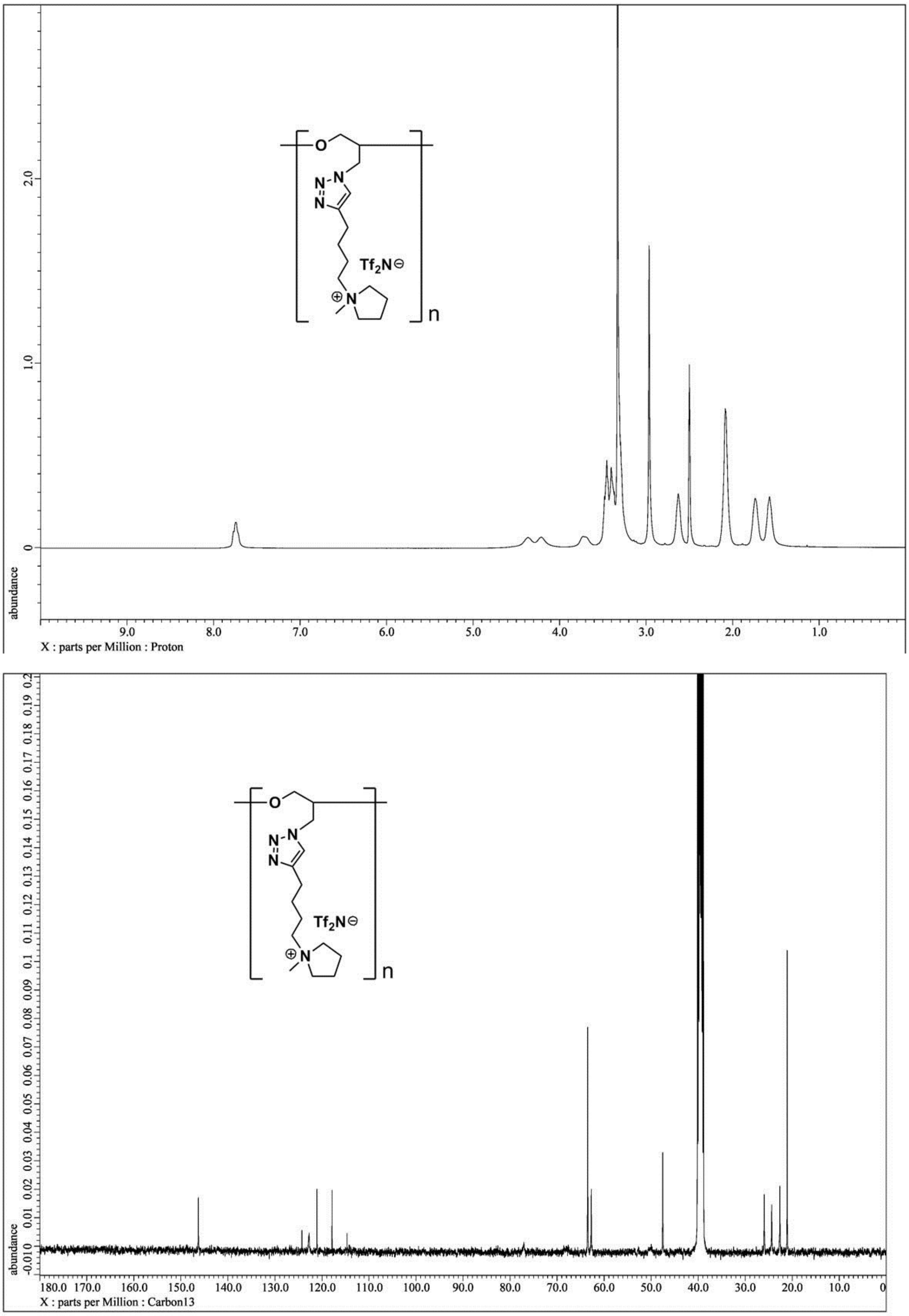

Figure S9. ^{1}H and ^{13}C NMR of **GTP-C4-Pyrro·Tf$_2$N** (DMSO-d_6).

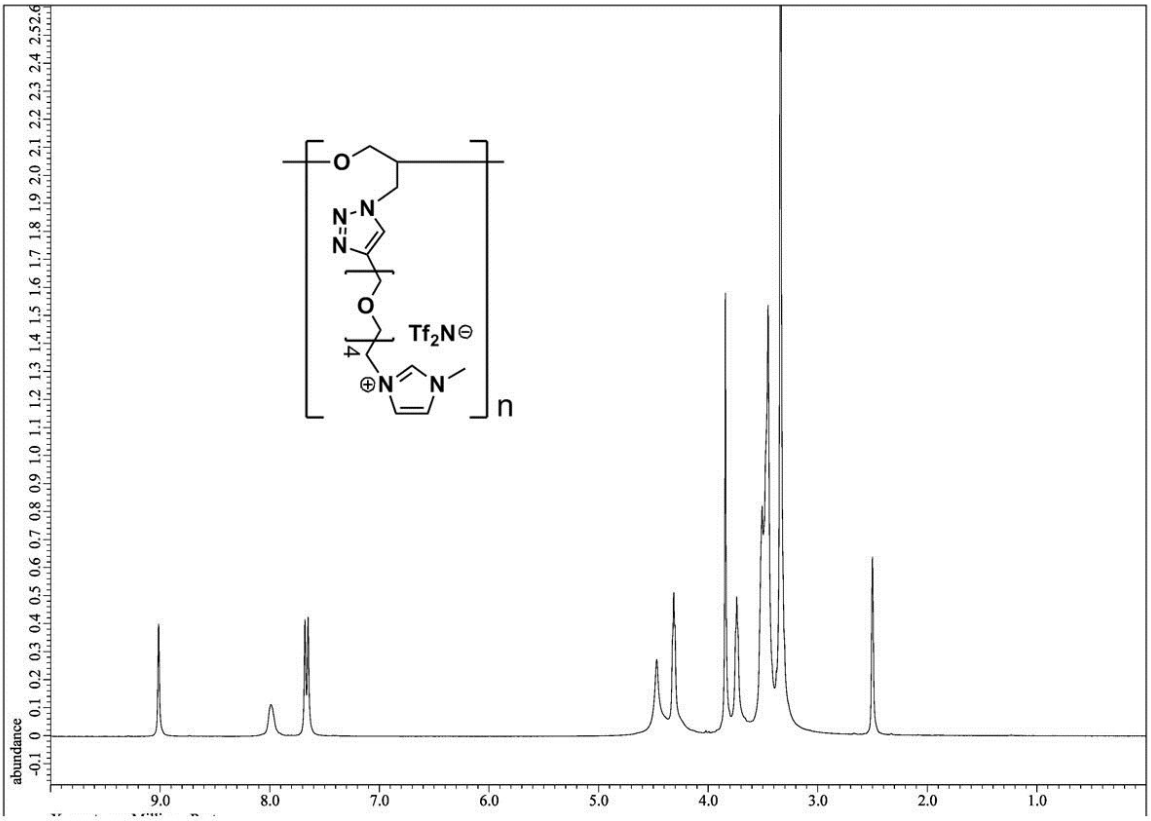

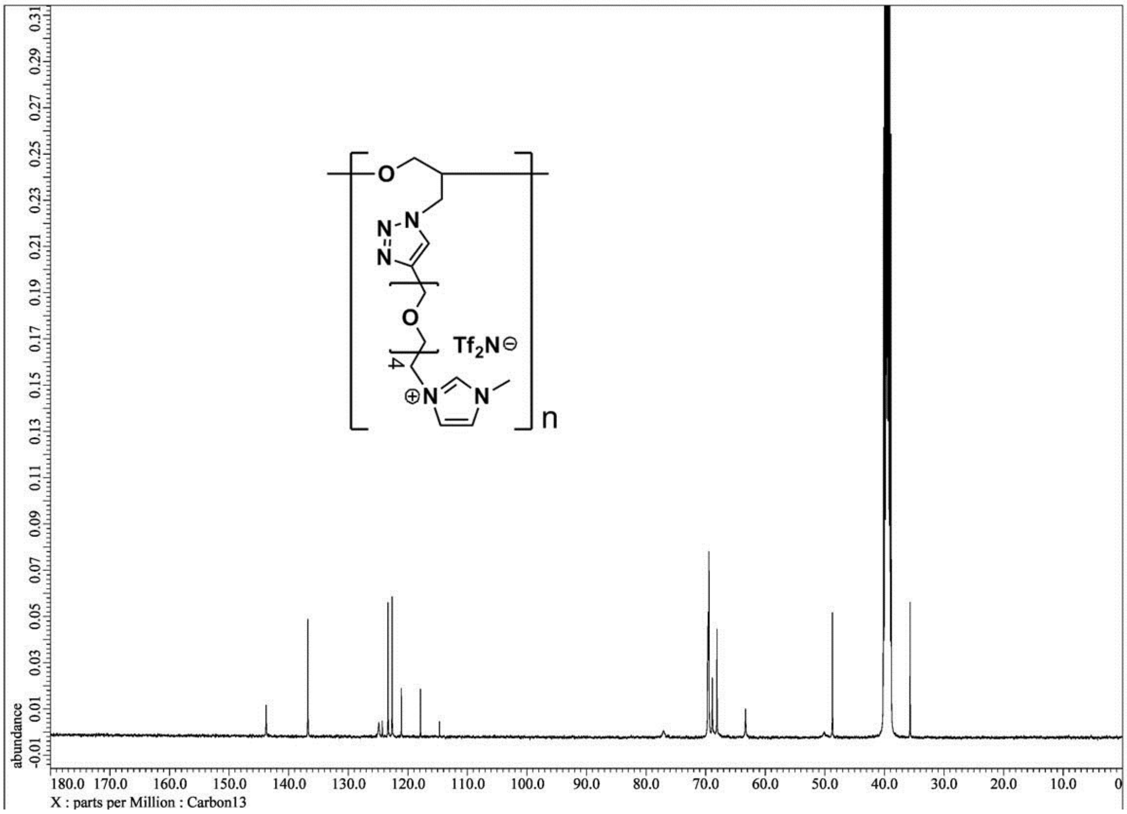

Figure S10. ^{1}H and ^{13}C NMR of **GTP-EG4-Im·Tf$_2$N** (DMSO-d_6).

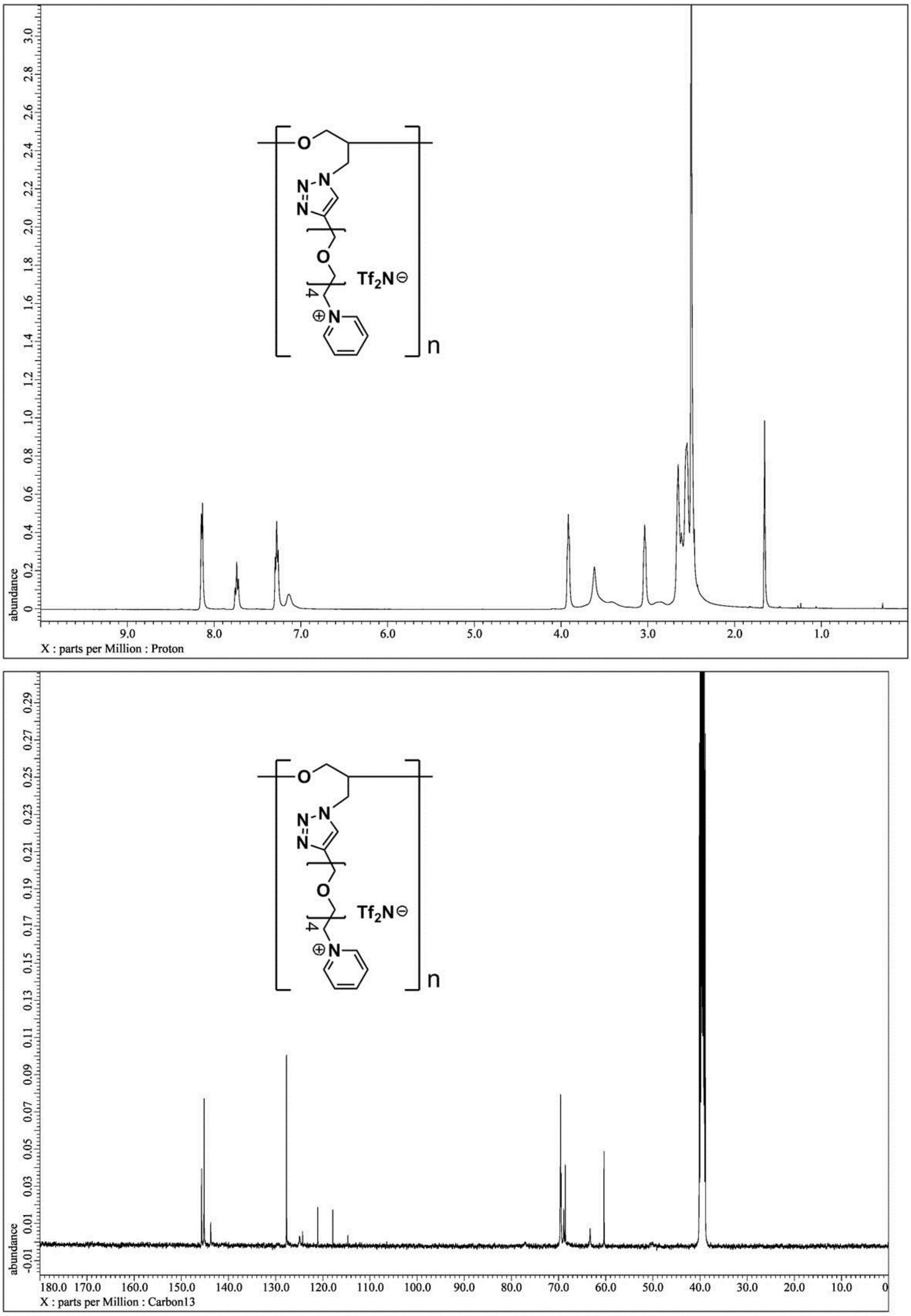

Figure S11. ^{1}H and ^{13}C NMR of **GTP-EG4-Pyri·Tf$_2$N** (DMSO-d_6).

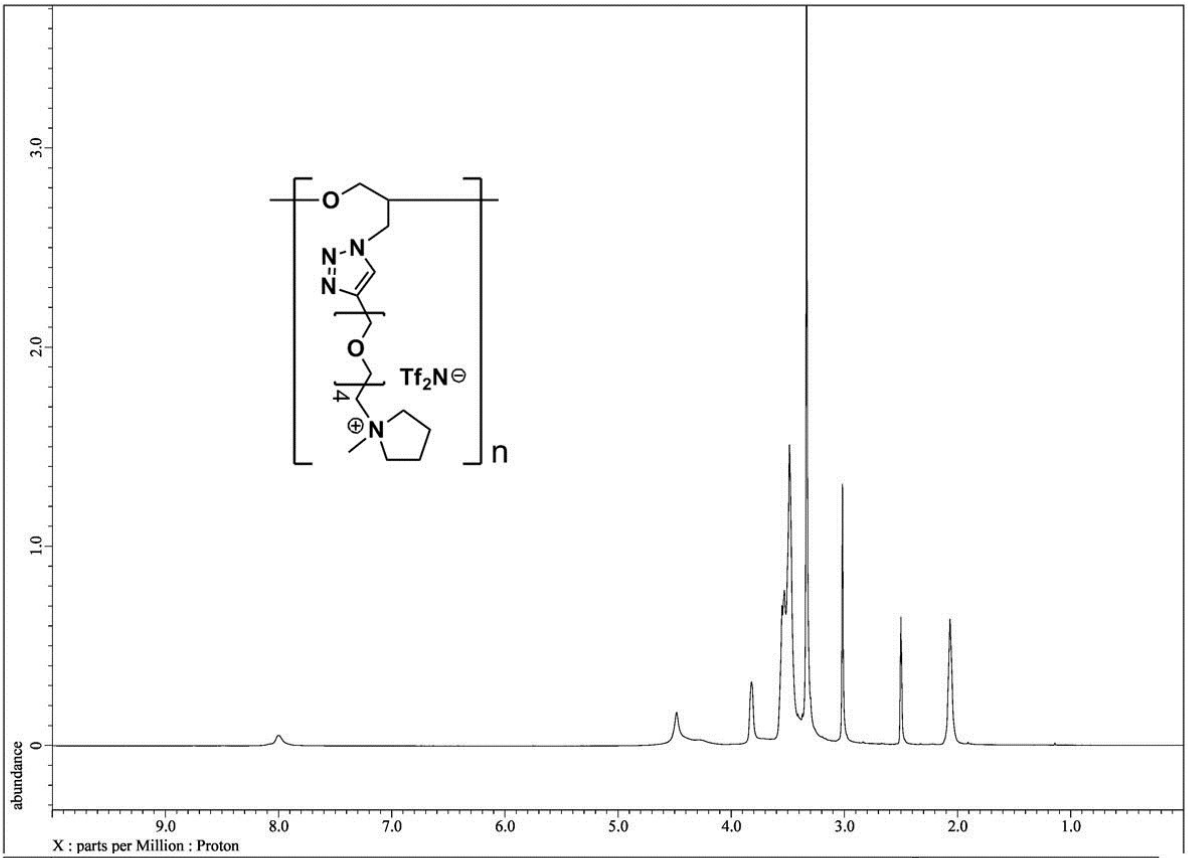

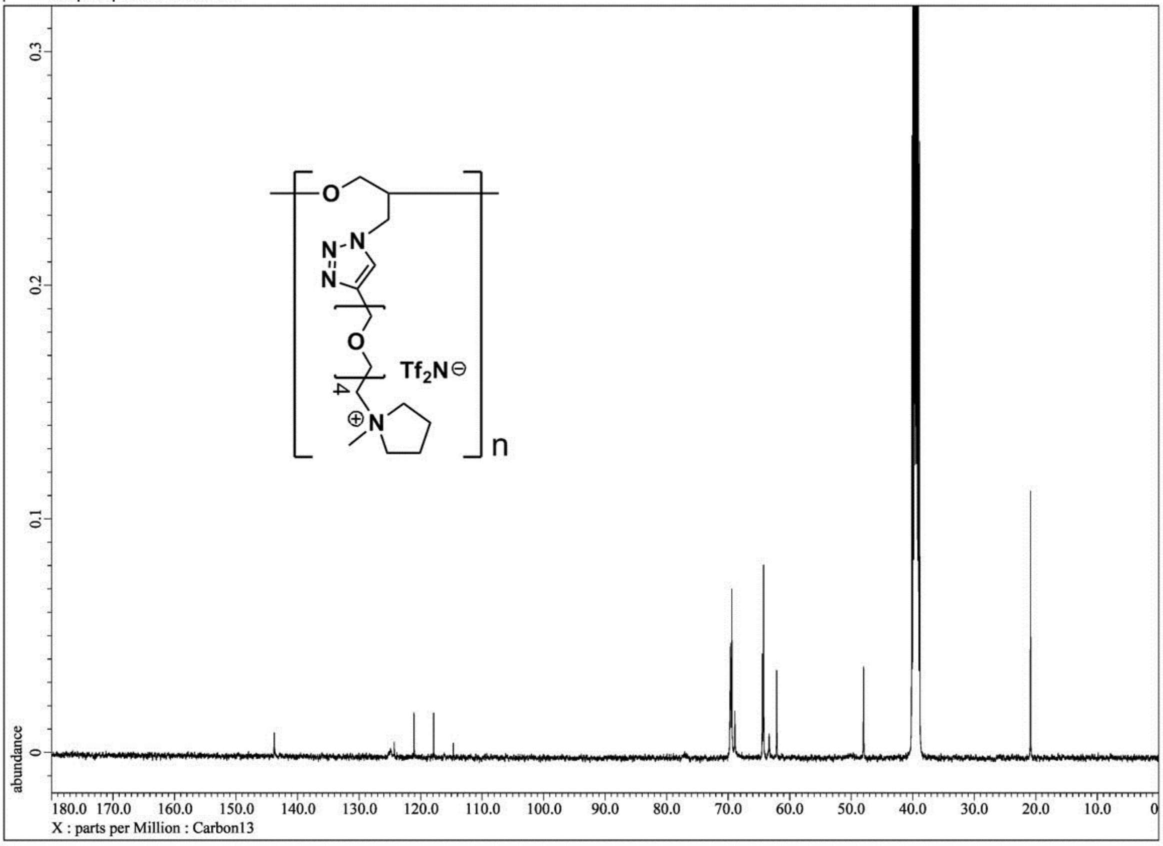

Figure S12. ^{1}H and ^{13}C NMR of **GTP-EG4-Pyrro·Tf$_2$N** (DMSO-d_6).

3. GPC measurement

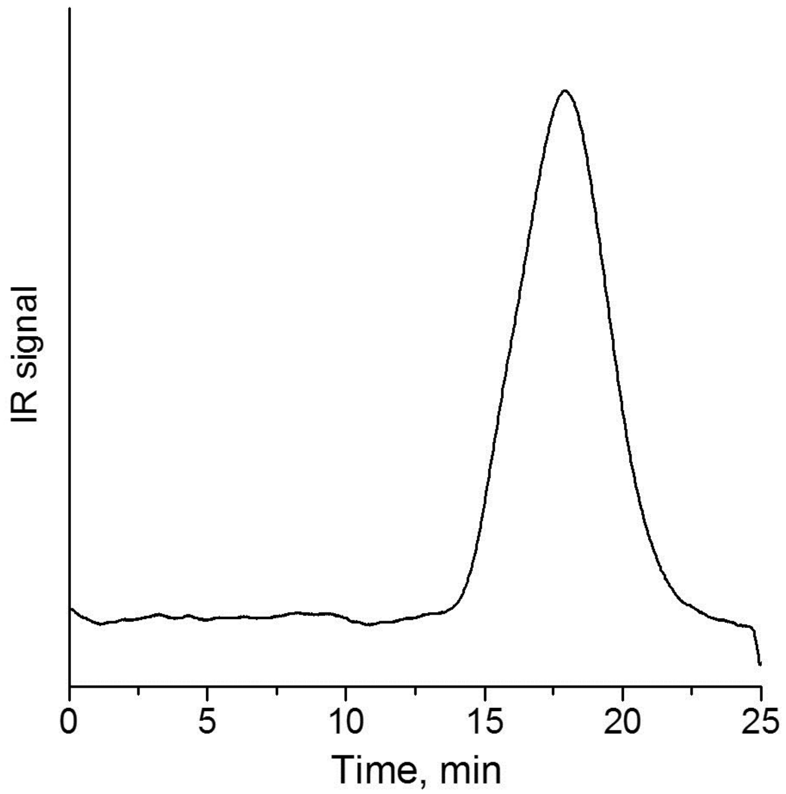

Figure S13 GPC chart of **GTP-C-Ph**.
M_n and M_w of **GTP-C-Ph** were determined to be 163 kDa and 319 kDa, respectively.

4. DSC measurements

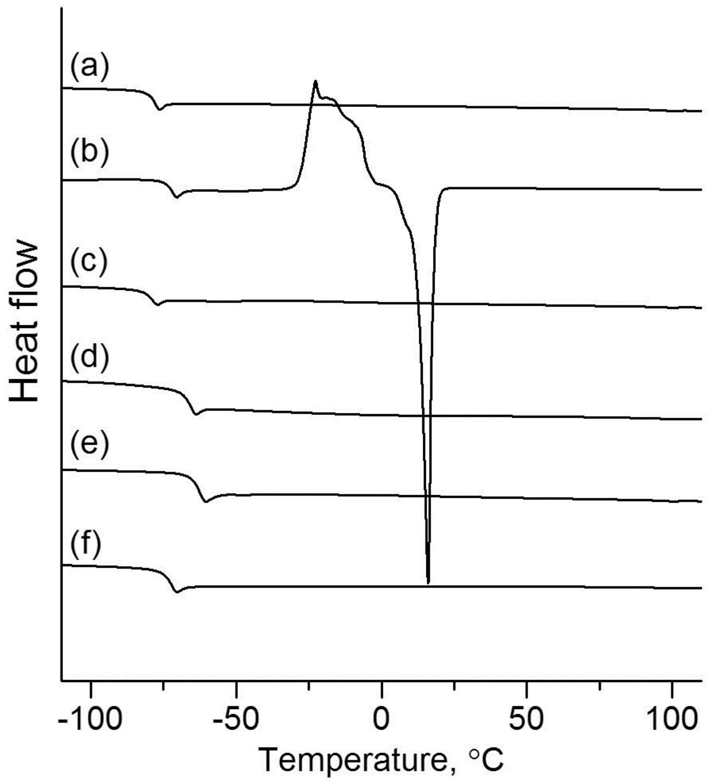

Figure S14 DSC traces of (a) **Im-C4-alkyne·Tf_2N**, (b) **Pyri-C4-alkyne·Tf_2N**, (c) **Pyrro-C4-alkyne·Tf_2N**, (d) **Im-EG4-alkyne·Tf_2N**, (e) **Pyri-EG4-alkyne·Tf_2N**, (f) **Pyrro-EG4-alkyne·Tf_2N**.

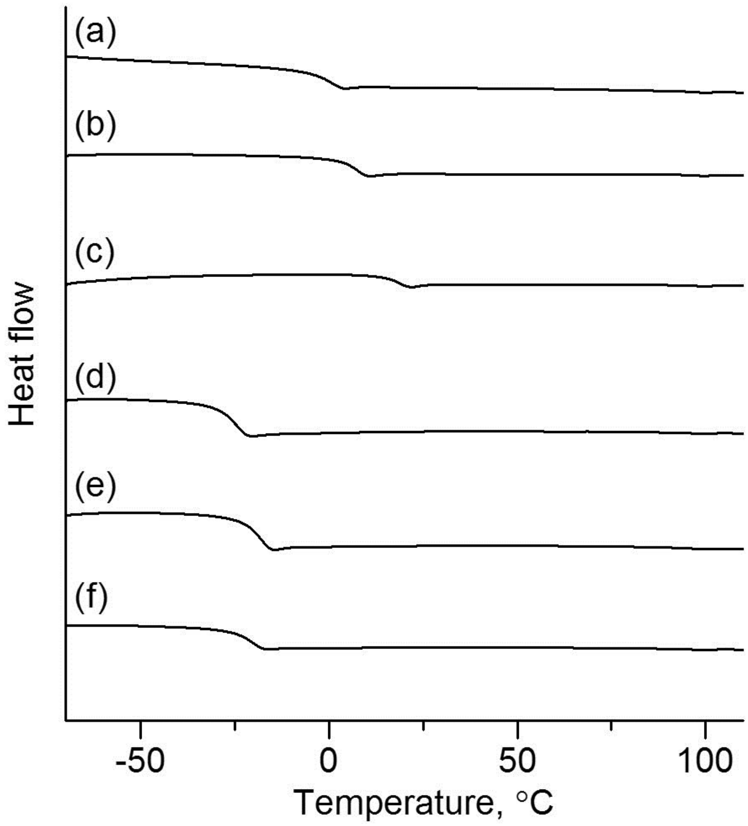

Figure S15 DSC traces of (a) **GTP-C4-Im·Tf$_2$N**, (b) **GTP-C4-Pyri·Tf$_2$N**, (c) **GTP-C4-Pyrro·Tf$_2$N**, (d) **GTP-EG4-Im·Tf$_2$N**, (e) **GTP-EG4-Pyri·Tf$_2$N**, (f) **GTP-EG4-Pyrro·Tf$_2$N**.

5. Thermal decomposition experiment

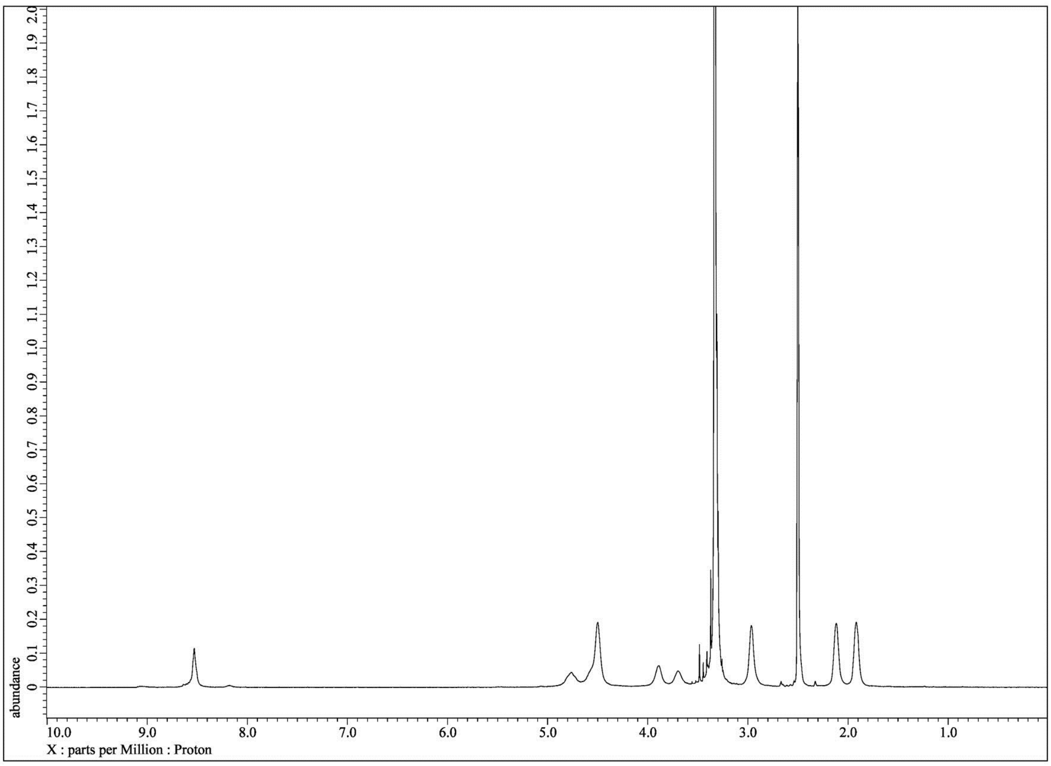

Figure S16 ^{1}H NMR spectrum of partially-decomposed **GTP-C4-Pyri·Tf$_2$N** (DMSO-d_6).

6. Impedance measurement

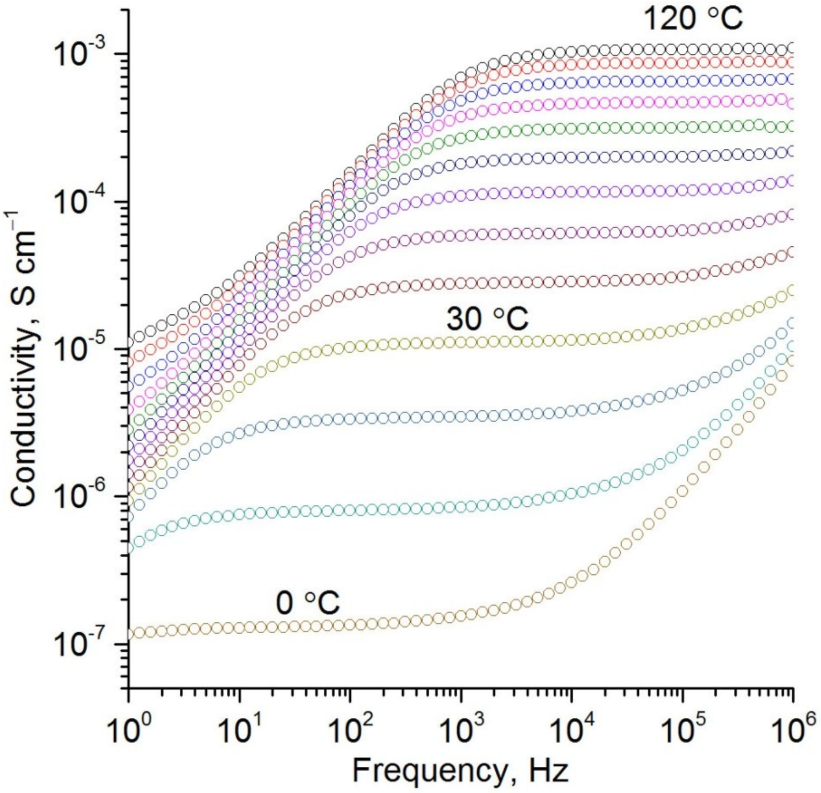

Figure S17 Conductivity vs frequency at temperatures from 0 °C to 120 °C for **GTP-EG4-Pyrro·Tf$_2$N**

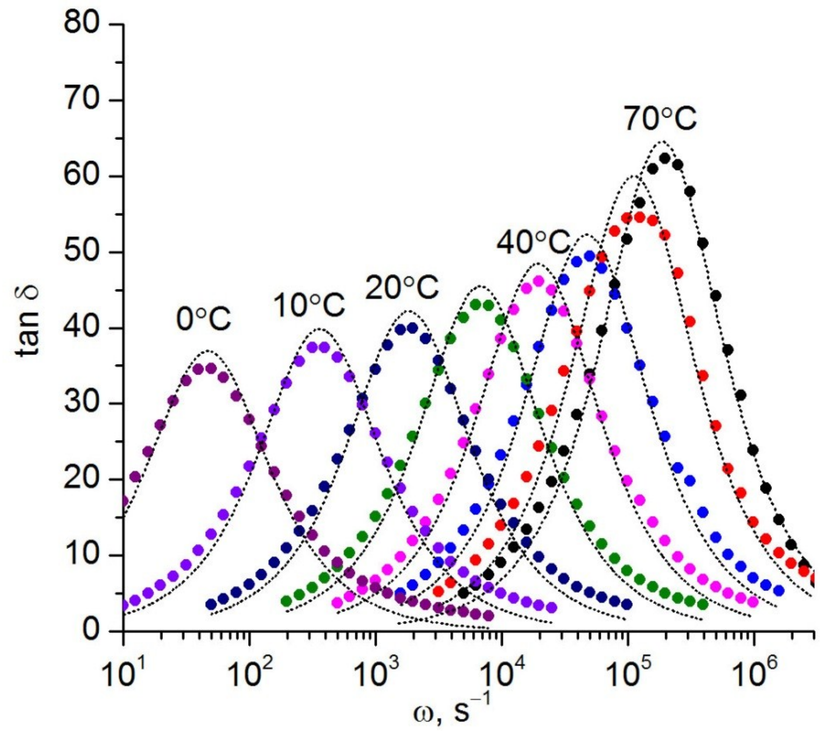

Figure S18 The plot of tan δ vs angular frequency from 0 °C to 70 °C for **GTP-EG4-Im·Tf$_2$N**. The dot curves were obtained from fitting by equation (2).

Table S1 Parameters of VFT equations for ionic conductivity and ion mobility (eqns. 1 and 6).

Cationic GTPs	σ_∞ S cm^{-1}	D_σ	T_σ K	μ_∞ cm^{2}V^{-1}s^{-1}	D_μ	T_μ K
GTP-C4-Im·Tf$_2$N	0.109	4.11	227	0.053	2.04	242
GTP-C4-Pyri·Tf$_2$N	0.113	3.23	240	0.069	1.14	265
GTP-C4-Pyrro·Tf$_2$N	0.060	3.45	239	0.021	1.26	262
GTP-EG4-Im·Tf$_2$N	0.076	3.72	218	0.030	1.79	232
GTP-EG4-Pyri·Tf$_2$N	0.148	3.93	220	0.046	1.12	250
GTP-EG4-Pyrro·Tf$_2$N	0.092	3.65	215	0.109	1.82	231